Saudi Pharmaceutical Journal 32 (2024) 102104

HOSTED BY

Contents lists available at ScienceDirect

Saudi Pharmaceutical Journal

journal homepage: www.sciencedirect.com

Original article

Formulation and evaluation of Fluconazole Nanosuspensions: In vitro characterization and transcorneal permeability studies

Basmah N. Aldosari *, Mohamed Abbas Ibrahim, Yara Alqahtani, Amal El Sayeh F. Abou El Ela

Department of Pharmaceutics, College of Pharmacy, King Saud University, Riyadh 11495, Saudi Arabia

ARTICLE INFO

Keywords:
Fluconazole
Nanosuspensions
Solvent evaporation
Stabilizers
Corneal permeation

ABSTRACT

The aim in this study was to develop and evaluate a nanofluconazole (FLZ) formulation with increased solubility and permeation rate using nanosuspensions. The FLZ nanosuspensions were stabilized using a variety of stabilizing agents and surfactants in various concentrations. The FLZ nanosuspension was characterized in vitro using particle size, zeta potential, X-ray powder diffraction (XRPD), and solubility. In addition, the ex vivo ocular permeation of FLZ through a goat cornea was analyzed. The results showed that the particle size of all nanosuspension formulations was in the nanometer range from 174.5 ± 1.9 to 720.2 ± 4.77 nm; that of the untreated drug was 18.34 μm. The zeta potential values were acceptable, which indicated suitable stability for formulations. The solubility of the nanosuspensions was up to 5.7-fold higher compared with that of the untreated drug. The results of the ex vivo ocular diffusion of the FLZ nanosuspensions showed the percentage of FLZ penetrating via the goat cornea increased after using Kollicoat to stabilize the nanosuspension formulation. Consequently, when using a nanosuspension formulation of Kollicoat, the antifungal activity of the drug strengthens.

1. Introduction

To effectively deliver hydrophobic drugs, nanosuspension technology has been developed. Pharmaceutical nanosuspensions are biphasic systems of nanometer-sized drug particles that are stabilized using a surfactant or polymer and administered orally, topically, parenterally, or pulmonarily. The particle size distribution of the solid particles in nanosuspensions is generally less than one micron, but can range between 200 and 600 nm (Muller, 2000; Savjani et al., 2012). Various methods can be used to prepare nanosuspensions, including media milling, precipitation, high-pressure homogenization in water or non-aqueous media, and a combination of precipitation and high-pressure homogenization (Chowdary & Madhavi, 2005; Patravale et al., 2004). The size of the particles, the viscosity of the medium, and the density of the particles, as described by Stokes' law, influence the rate of deposition of the nanoparticles in a nanosuspension (Nutan and Reddy, 2010). Nanosuspensions are unstable because of particle growth and nucleation, which are due to their high surface area; they are also thermodynamically unstable due to agglomeration and crystal growth. Because nanosuspensions must be stable to prevent the aggregation of molecules that have large kinetic energy, stabilizers must be used. However, different drugs require different stabilizers: no single stabilizer can be used for all medicinal product preparations. No guideline or rule is available for the selection of an appropriate stabilizer. As such, a simple trial-and-error approach must be followed (Wang et al., 2013). Some of the stabilizers that are used include polyvinyl pyrrolidone (PVP), polyvinyl alcohol (PVA), hydroxypropyl methyl cellulose (HPMC), hydroxypropyl methyl cellulose (HPC), polyethylene glycol (PEG), polyethylene imine (PEI), Tween, and block copolymers of polyethylene oxide-polypropylene oxide known as Pluronics (Wang et al., 2013). To ensure the electrostatic stability of a formulations, the stabilizer should adsorb onto the nanosuspension surface of the drug particle. Naproxen nanosuspensions prepared via anti-solvent precipitation were stabilized using PVP K15 and Pluronic F127 (X. Chen, Matteucci, Lo, Johnston, & Williams III, 2009). Gupta et al. formulated forskolin nanosuspensions stabilized with Pluronic F127 using a wet crushing technique (S. Gupta, Samanta, & Raichur, 2010).

Fluconazole (FLZ) is a solid antifungal that belongs to the triazoles. A wider antifungal spectrum and less toxicity than isolated amphotericin B were observed when FLZ was subconjunctivally administered in association with topical amphotericin B (Mahdy et al., 2010). Yilmaz and Maden (Yilmaz & Maden, 2005) successfully treated 60 % of cases of

* Corresponding author at: Department of Pharmaceutics, College of Pharmacy, King Saud University, Riyadh 11495, Saudi Arabia.
E-mail addresses: baldosari@ksu.edu.sa (B.N. Aldosari), mhamoudah@KSU.EDU.SA (M.A. Ibrahim), alqahtani.yara@gmail.com (Y. Alqahtani), aelsaih@ksu.edu.sa (A.E.S.F. Abou El Ela).

https://doi.org/10.1016/j.jsps.2024.102104
Received 3 April 2024; Accepted 15 May 2024
Available online 16 May 2024

fungal keratitis with subconjunctival injections of FLZ alone.

Nanotechnology is currently widely used as a treatment strategy in the management of ophthalmologic disorders that affect the anterior and posterior sections of the eye. Ocular nanocarriers are capable of the selective, targeted, and sustained release of molecules to a site (Wadhwa et al., 2009). Ocular drugs that can be delivered via nanotechnology include liquid dosage forms such as microemulsions and nanosuspensions; particulate carriers such as microparticles, polymerics, and lipid nanoparticles; vesicular carriers such as liposomes and niososmes; and many others such as dendrimers, hydrogel systems, prodrugs, and nanocarriers (Wadhwa et al., 2009). With ophthalmic applications, the particle size should not exceed a certain size to avoid the scratching sensation in the eyes that occurs with larger particles. Patient comfort during administration is increased as the particle size of the ocular drug decreases (Sayed et al., 2015; Zimmer & Kreuter, 1995).

In this study, the primary objective was to increase the ocular efficacy of FLZ via the nanonization of drug particles to increase its permeation permeability. Antisolvent precipitation nanonization techniques used to prepare FLZ nanosuspensions, and the influence of different types and concentrations of stabilizers was studied via the characterization of the FLZ nanosuspensions in terms of particle size, zeta potential, X-ray powder diffraction (XRD), and solubility. In addition, the transocular permeation of the FLZ nanosuspensions into goat cornea was studied ex vivo.

2. Materials and methods

2.1. Materials

The FLZ was obtained as a gift from the Aljazerah Pharmaceutical Company (Riyadh, Saudi Arabia). Low-viscosity hydroxypropyl methylcellulose (LV HPMC, grade E3) was purchased from Dow Chemical Co. (Midland, MI, USA). Kollicoat IR (KL) was obtained from BASF (Ludwigshafen, Germany). Pluronic F127 (PLF127) was purchased from C.H. (Erbesloh, Krefeld, Germany); xanthan gum (XG) was bought from Sigma Chemical Co. (MO, USA). All other materials, solvents, and reagents were of analytical grade, which were used without further purification.

2.2. Methods

2.2.1. UV spectrophotometry assay of FLZ

A stock solution of FLZ was prepared by weighing 100 mg of FLZ and transferring it to a 100 ml volumetric flask; the remainder of the volume was methanol. Serial dilutions of 40, 80, 120, 160, 200, 240, and 280 μg/mL were prepared from the stock, which were added to a 10 ml volumetric flask. Phosphate buffer, pH 7.4, was added as the remainder of the volume. A calibration curve was constructed by determining the absorbance at 260 nm of the resulting samples (Göğer and Aboul-Enein, 2001). The experiments were conducted in triplicate, and the average absorbance was plotted against the corresponding concentration to construct the calibration curve (Helal et al., 2012).

2.2.2. Preparation of the FLZ nanosuspensions

During the preliminary studies, the concentrations of the drug and stabilizers and the speed of stirring were optimized to produce FLZ nanosuspensions with small particles and higher zeta potentials to prevent aggregation. Different stabilizers were used to prepare the FLZ nanosuspensions, including PLF127, KL, HPMC, and XG. The nanonization conditions were kept constant during the whole experiment. The FLZ nanosuspensions were prepared via the antisolvent evaporation method. An accurately weighed 100 mg of FLZ was dissolved in 3 ml of dichloromethane. Then, the drug was dropped using a syringe into 20 ml of distilled water containing the stabilizer (0.5, 1, or 5 w/v %) under magnetic stirring at 1000 rpm for 4 h until the solvent was completely evaporated. This resulted in a supersaturation of the FLZ in solution and the formation of the nanosuspension. The prepared FLZ nanosuspensions were then stored at 4°C until used for characterization (Abou El Ela et al., 2021).

2.2.3. Evaluation of prepared FLZ nanosuspensions

2.2.3.1. Determination of particle size and zeta potential. The mean particle size and zeta potential of the freshly prepared nanosuspensions were determined via photon correlation spectroscopy (PCS) using a Zetasizer (Nano ZS, Malvern Instruments, UK) at room temperature. The samples were adequately diluted with deionized water (1: 1000) and placed in an electrophoretic cell. All examinations were in triplicate.

2.2.3.2. X-ray powder diffraction (XRPD). The prepared FLZ nanosuspensions were frozen at −30°C and dried using a freeze-dryer (Martin Christ, Osterode, Germany) at −40°C. The XRPD analysis of the pure drugs and freeze-dried nanoparticle samples was conducted using a Ultima IV diffractometer (Rigaku Inc. Tokyo, Japan) over the $3 - 60^{\circ}\ 2\theta$ range at a scan speed of 1°/min. The tube anode was Cu, at Ka = 0.1540562 nm, monochromatized with graphite crystal (Rigaku Inc. Tokyo, Japan). The analysis was performed at a 40 kV of tube voltage and a 40 mA tube current in step scan mode (step size 0.02°, 1 s per step). This analysis was performed to determine the crystallinity of the pure drugs in the freeze-dried nanoparticles (Ibrahim, 2014).

2.2.3.3. Solubility. Saturation solubility studies were conducted for both the untreated drug and the lyophilized nanoparticles in the formulated nanosuspensions. A total of 10 mg of both FLZ and FLZ nanoparticles, equivalent to 10 mg of FLZ, was weighed and placed in separate stoppered conical flask composed of 5 mL phosphate buffer (pH 7.4). The flasks were placed in a water bath shaker (37 °C ± 0.5) at 100 rpm for 72 h. Then, each 0.5 mL aliquot was withdrawn and filtered through a 0.22 μm Millipore filter. An aliquot of 100 μL of each filtrate was diluted with phosphate buffer pH 7.4 and assessed using a UV spectrophotometer at 260 nm. Each experiment was carried out in triplicate, the average saturation solubility of FLZ was determined in mmol/mL, and the standard deviation was calculated.

2.2.3.4. Transmission electron microscopy (TEM). Transmission electron microscopy (TEM) was performed to evaluate the morphological characteristics and size of the particles in the FLZ nanosuspensions. The nanoparticle suspension of the selected formula was dropped onto carbon-coated copper grids for viewing with a transmission electron microscope (jem-1400, JEOL Ltd., Tokyo, Japan). Imaging viewer software was used for image capture and analysis.

2.2.4. Ex vivo transcorneal permeation

Goat corneas were used to study the permeation of the developed formulations across the corneal membrane. Whole goat eyeballs were obtained from a slaughterhouse and transported to the laboratory in normal saline maintained at 4 °C. The corneas were carefully removed along with 5–6 mm of the surrounding scleral tissue, which were then washed with cold saline. The washed corneas were kept in a cold, freshly prepared tear buffer solution at pH 7.4 (Pathak et al., 2013; Abou El Ela et al., 2021). The ex vivo release study of FLZ nanosuspension formulations was performed in 12 mL of the buffered solution (pH 7.4) as the receptor medium at 37 ± 0.5 °C and 100 rpm using the Franz diffusion method (Logan instruments, NJ, USA). Using the diffusion cell at pH 7.4, 1 g of each nanosuspension formulation with 0.5 % w/w FLZ was placed on the goat corneal membrane. Caution was taken to ensure that the corneal membrane only touched the receptor medium surface. The whole system was kept at 37 ± 0.5 °C and stirred at 100 rpm. The sink condition was kept during the ex vivo permeation study. Aliquots of 1 ml were withdrawn at different time intervals (1, 2, 4, and 6 h) and exchanged with an equivalent quantity of fresh buffer solution. All

samples are filtered through a 0.22 μm pore Millipore membrane filter and assayed at a λ_{max} of 260 nm using a UV spectrophotometer (Cambridge, England). All tests were performed with triplicate.

2.2.5. Statistical analysis

ANOVA was used to calculate the P values for a given variable. Fisher's least significant difference (LSD) test was used (with this method, a 5.0 % risk of calling each pair of means is considered meaningfully different when the real difference equals 0) to identify the significant differences between variables.

3. Results

3.1. UV spectrophotometry assay of FLZ

The standard calibration curve of the pure FLZ in the phosphate buffer solution (pH 7.4) is show in Fig. 1. Different concentrations of the pure medicinal drug product, ranging from 40 to 280 μg/mL, were prepared in pH 7.4 phosphate buffer, and the absorbances were spectrophotometrically determined at 260 nm. The resulting standard calibration curve was linear for the considered concentration range and obeyed the Beer–Lambert principle, with a correlation coefficient (R^2) of 0.9990.

3.2. Characterization of prepared FLZ nanosuspensions

3.2.1. Particle size distribution and zeta potential measurements

Table 1 shows the particle size, zeta potential, and solubility of all FLZ nanosuspension formulations that were successfully prepared and stabilized with different stabilizers. The particle sizes of the FLZ nanosuspensions stabilized by with 0.5 %, 1 %, and 5 % w/v of PL were 174.5, 354.9, and 192.5 nm, respectively, with PDI values ranging from 0.45 to 0.69. The zeta potentials of these nanosuspensions were −35.5 mv, −30.3, and −35.8 mv, respectively. For our FLZ nanosuspensions, the stabilizer (KL) concentration noticeably impacted the particle size of the produced nanosuspensions. The particle sizes of the FLZ nanosuspensions stabilized with 0.5 %, 1 % and 5 % w/v of KL were 250.2, 445.4, and 199.3 nm, respectively, with PDI values ranging from 0.26 to 0.32, as shown in Table. The zeta potentials of these nanosuspensions were −21.4, −25.5, and −24.4 mv, respectively. The results showed that the HPMC polymer had the ability to produce FLZ nanosuspensions with small particles (249.9–374.6 nm), as shown in Table 1. In addition, the zeta potential values of these nanosuspensions were −37.3 and −30.1 mv. When a high concentration (5 %) of HPMC was added, determining the particle size and zeta potential of the nanosuspension was challenging due to its high viscosity (Alshora et al., 2018). The addition of XG polymer produced nanosuspensions with relatively large particles. Increasing the XG concentration from 0.5 % to 1 % reduced particle size of the nanosuspension from 720.2 ± 4.77 to 685 ± 0.52 nm, with zeta potential values of –39.8 and −35.6 mV, respectively, as shown in Table 1.

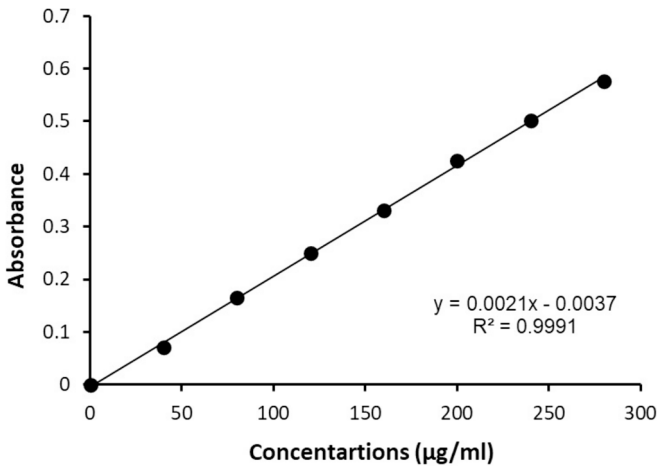

Fig. 1. Calibration curve of FLZ in pH 7.4 phosphate buffer determined at 260 nm. The experiments were carried out in triplicate.

Table 1
Characterization of the different formulations of FLZ nanosuspensions (n = 3, mean ± SD).

Formulation	FLZ nanosuspension			
	Particle size (nm)	PDI	Zeta potential (Mv)	Drug solubility (mmol/L)
F 1 (PLF 127 0.5 %)	174.5 ± 1.9	0.558	−35.5	3.4 ± 0.009
F 2 (PLF 127 1 %)	354.9 ± 3.6	0.69	−30.3	2.5 ± 0.539
F 3 (PLF 127 5 %)	192.9 ± 0.5	0.453	−35.8	3.7 ± 0.808
F 4 (KL 0.5 %)	250.2 ± 0.17	0.324	−21.4	6.8 ± 1.418
F 5 (KL 1 %)	445.4 ± 0.53	0.455	−25.5	2.9 ± 0.440
F 6 (KL 5 %)	199.3 ± 0.78	0.264	−24.4	1.8 ± 0.036
F 7 (HPMC 0.5 %)	374.6 ± 0.77	0.366	−37.3	3.7 ± 0.332
F 8 (HPMC 1 %)	249.9 ± 0.17	0.272	−30.1	2.2 ± 0.350
F 9 (HPMC 5 %)	N/A			
F 10(XG 0.5 %)	720.2 ± 4.77	0.602	−39.8	1.8 ± 0.080
F 11 (XG 1 %)	685 ± 0.52	0.597	−35.6	4.2 ± 0.180
F 12 (XG 5 %)	N/A			

*Particle size of FLZ raw powder was 18.34 μm; ** solubility of untreated FLZ was 1.2 ± 0.215 mmol/L.

3.2.2. Solubility

Table 1 shows the aqueous solubility of the raw FLZ and freeze-dried FLZ nanoparticles in the nanosuspensions stabilized with different concentrations of different stabilizers at 37 °C. The untreated FLZ exhibited an aqueous solubility of 1.2 ± 0.21 mmol/L. In comparison with the untreated drug, the FLZ nanosuspensions were substantially more water soluble. The drug exhibited a remarkable increase in its solubility in case of nanoparticles stabilized by PL F127, and a higher solubility (3.7 ± 0.808 mmol/L) was obtained using 5 % stabilizer concentration. Table 1 shows the aqueous solubility of the raw FLZ and FLZ nanoparticles stabilized with different KL concentrations. The aqueous solubility of the freeze-dried FLZ nanosuspensions was higher than that of the untreated drug. The measured drug solubility in the nanosuspensions stabilized with 0.5 %, 1 % and 5 % w/v of KL was 6.8 ± 1.418, 2.9 ± 0.440, and 1.8 ± 0.036 mmol/L, respectively. The measured solubility was 3.7 ± 0.33 and 2.2 ± 0.35 mmol/L for FLZ nanosuspensions stabilized with 0.5 % and 1 % w/v HPMC, respectively. The drug solubility was 1.8 ± 0.08 and 4.2 ± 0.18 mmol/L for the nanosuspensions stabilized with 0.5 % and 1 % w/v of XG, respectively.

3.2.3. X-ray powder diffraction (XRPD)

The X-ray diffraction spectra of the raw FLZ and freeze-dried FLZ nanosuspension formulations stabilized with different stabilizers were obtained to evidence changes in the solid state. The occurrence of a number of well-defined peaks in the X-ray spectrum of FLZ revealed that the drug is a crystalline material with representative diffraction peaks at 2θ angles of 5.98, 5.12, 4.53, 3.63, 3.32, 3.05, and 2.85 Å. Furthermore, two characteristic peaks were observed for the PL copolymers at 19.2 and 20.4 Å, as shown in Fig. 2.

The intensities of the characteristic diffraction peaks of FLZ were slightly lower for the freeze-dried FLZ nanosuspensions containing 0.5 KL; however, for the FLZ nanosuspension stabilized with 1 % KL, the drug diffraction peaks completely disappeared as shown in Fig. 3.

The XRPD spectra of the FLZ, HPMC, and freeze-dried FLZ nanosuspensions stabilized with 0.5 (F7) and 1 % (F8) HPMC are shown in

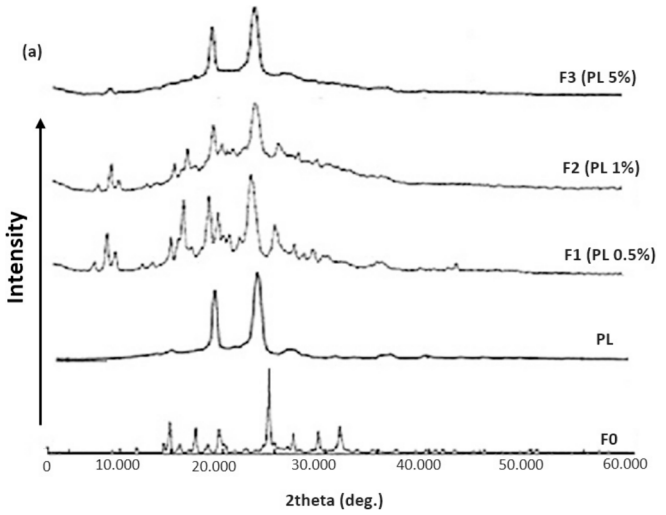

Fig. 2. X-ray powder diffraction of FLZ nanosuspensions stabilized by PL F 127 stabilizer compared to the individual components. F0 (Untreated FLZ).

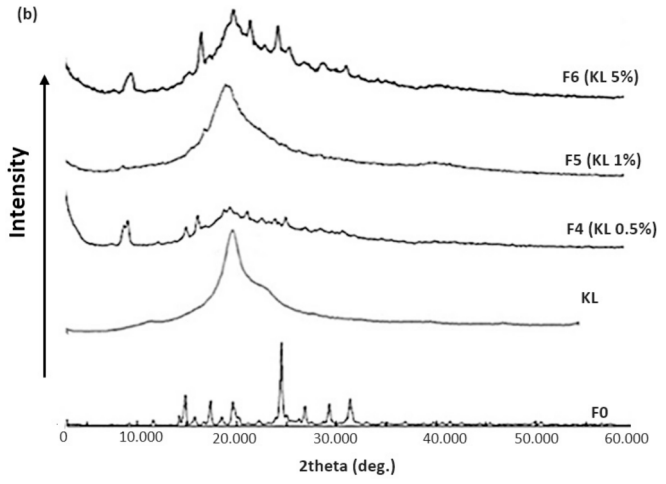

Fig. 3. X-ray powder diffraction of FLZ nanosuspensions stabilized KL stabilizer compared to the individual components. F0 (Untreated FLZ).

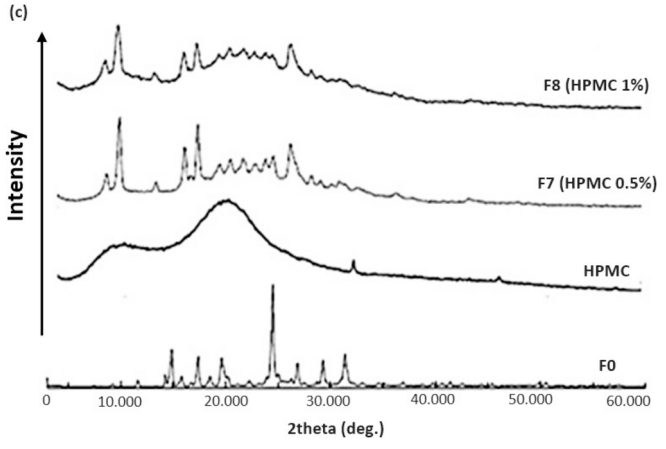

Fig. 4. X-ray powder diffraction of FLZ nanosuspensions stabilized by HPMC compared to the individual components. F0 (Untreated FLZ).

Fig. 4. The characteristic X-ray diffraction peaks of FLZ were found at their original intensities in the FLZ nanosuspension formulations. However, FLZ in its crystalline form was revealed by the presence of FLZ diffraction peaks in the XRPD spectra.

The XRPD spectra of FLZ, XG, and FLZ nanosuspensions stabilized with 0.5 (F10) and 1 % (F11) XG after freeze-drying are shown in Fig. 5.

3.3. Ex vivo transcorneal permeation study

The selected FLZ nanosuspensions stabilized with PLF 127, KL, HPMC, and XG exhibited widely different permeation patterns, and permeation was high through the freshly excised goat cornea. In particular, after 6 h, the FLZ nanosuspension stabilized with KL (F4) significantly increased ($P < 0.05$) the percent of drug that permeated the corneas relative to that of the FLZ nanosuspension containing PLF 127 (F3), for which the lowest drug permeation percentage was recorded. After 6 h, the drug permeation of the F4 nanosuspension stabilized with KL was 100.4 ± 9.0 % whereas that of the F3 nanosuspension stabilized with PLF 127 was 61.8 ± 2.4 % (Fig. 6). The cumulative drug permeations of formulations F11, stabilized with XG, and F7, stabilized with HPMC, were higher, at 75.9 ± 2.6 and 70.7 ± 1.5 %, respectively, than that of F3 (61.8 ± 2.4 %) after 6 h due to their higher solubility.

The goat corneal permeation parameters for F3 (5 % PLF 127), F4 (0.5 % KL), F7 (0.5 % HPMC), and F11 (1 % XG) were calculated and are listed in Table 2. The coefficient of determination (R^2) of the regression lines can be used to evaluate the stability of drug permeation. The nearer the value of R^2 is to 1, the greater the improvement in the stability of the steady-state flux (J_{SS}). Corresponding to Table 2, the R^2 values of F3 (5 % PLF 127), F4 (0.5 % KL), F7 (0.5 % HPMC), and F11 (1 % XG) ranged from 0.926 to 0.993, indicating the stability of the steady-state flux (J_{ss}) of 200.137 ± 1.284 to 162.428 ± 9.034 μg/cm^2/h. The lag times of the selected FLZ nanosuspensions wee all short, ranging from 0.018 ± 0.01 to 0.894 ± 0.078 h. The transcorneal permeation flux (J_{ss}) of FLZ from the F3 (5 % PLF 127), F4 (0.5 % KL), F7 (0.5 % HPMC), and F11 (1 % XG) nanosuspensions were 162.428 ± 9.034, 260.630 ± 17.529, 200.137 ± 1.284, and 230.069 ± 3.623 μg/cm^2/h, respectively. Furthermore, the cumulative amount of the drug permeated after 6 h (μg/cm^2) of the selected formulations ranged from 1749.15 ± 0.117 to 2841.45 ± 0.451, respectively for F3 and F4.

4. Discussion

FLZ nanosuspensions were successfully prepared using different concentrations of stabilizers. The effects of these stabilizers on the nanoparticle size and zeta potential of the nanosuspensions varied with

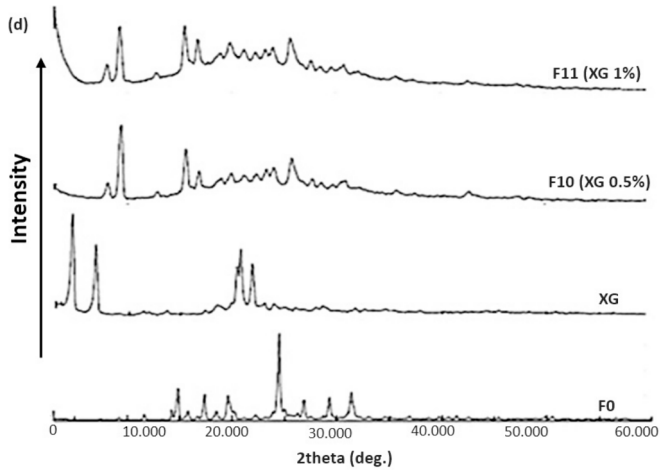

Fig. 5. X-ray powder diffraction of FLZ nanosuspensions stabilized by XG compared to the individual components. F0 (Untreated FLZ).

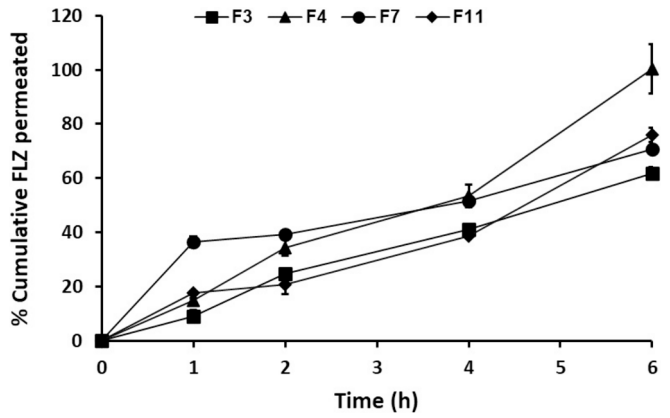

Fig. 6. Ex vivo goat cornea permeation of FLZ nanosuspension formulations (n = 3, mean ± SD).

Table 2
Ex vivo transcorneal permeation parameters of FLZ in different nanosuspension formulations (n = 3, mean ± SD).

Nanosuspension formulation	Cumulative drug permeated after 6 h (μg/cm^2)	Flux, J_{ss} (cm^2/h)	Permeability coefficient, K_p (x10^3 cm/h)	Lag time (h)	R^2
F 3 (PLF 127 5 %)	1749.15 ± 0.117	162.428 ± 9.034	32.486 ± 1.807	0.125 ± 0.185	0.993 ± 0.006
F4 (KL 0.5 %)	2841.45 ± 0.451	260.630 ± 17.529	52.126 ± 0.003	0.124 ± 0.075	0.981 ± 0.020
F7 (HPMC 0.5 %)	2001.69 ± 0.001	200.137 ± 1.284	40.020 ± 0.255	0.018 ± 0.010	0.926 ± 0.001
F11 (XG 1 %)	2168.74 ± 0.078	230.069 ± 3.623	46. 014 ± 0.725	0.089 ± 0.078	0.988 ± 0.006

stabilizer concentration and type. The addition of Pluronic F127 ensured the creation of nano-sized particles in the FLZ nanosuspensions. Increasing the concentration of the stabilizer from 1 % to 5 % significantly decreased ($P < 0.05$) the nanoparticle size of the FLZ nanosuspensions. However, increasing the concentration of PLF from 0.5 % to 1 % did not produce the same results. Alshora et al. (Alshora et al., 2020) reported that PLF127 concentration showed a slight effect on the size of pioglitazone HCl nanoparticles prepared via wet milling. Polymeric stabilizers such as PL, KL, HPLC, and XG increase nanosuspension stability via adsorption to the surface of the nanoparticles, thereby producing steric repulsion amongst particles and increasing nanosuspensions viscosity to prevent aggregation processes (Xue and Sethi, 2012).

The drug solubility remarkably increased when stabilized with PLF127, and a higher solubility (3.7 ± 0.808 mmol/L) was obtained using 5 % PLF127. This may have been due to the smaller particles in the FLZ nanosuspensions, which, in turn, increased the surface area, leading to increased drug solubility (Zu et al., 2012). In addition, PLF 127 is a nonionic surfactant that increases the aqueous solubility of several drugs in the form of a micellar solubilizing powder (Kabanov & Alakhov, 2002; Sezgin et al., 2006). Furthermore, no significant difference was found in the drug solubility as the FL F127 concentration was increased from 0.5 to 5 %. Increasing the HPMC concentration increased solution viscosity and, in turn, the coating of the nanoparticles formed during the solvent evaporation phase, resulting in larger particles (Ramezani et al., 2014). The enlargement in the particle size with increasing HPMC concentration could also have been due to the insufficient amount of polymer available to cover the new, larger surface of particles due to the increased; at this point, agglomeration can occur and decrease solubility (Alshora et al., 2018). The drug solubility was lower when using 0.5 % XG as the nanosuspension stabilizer, which we attributed to the large nanoparticles produced at this concentration. XG may be involved in the self-wetting of FLZ, increase the stability of FLZ due to its hydrophilic nature (Comba, Dalmazzo, Santagata, & Sethi, 2011; Comba & Sethi, 2009; Xue & Sethi, 2012). The FLZ nanosuspension stabilized with 5 % XG was too viscous to be characterized in further studies.

The characteristic diffraction peaks of FLZ were slightly less intense for the freeze-dried FLZ nanosuspensions containing 0.5 and 1 % PLF127; however, the drug diffraction peaks in the FLZ nanosuspensions stabilized with 5 % PL completely disappeared. In these nanosuspensions, the results of the XRPD studies showed that FLZ was homogeneously dispersed in the PL matrices and transformed to its amorphous form (Suzuki et al., 1996). The results agree with those of Ibrahim et al. (2018), who showed that the crystalline structure of docetaxel changes in nanoparticles loaded with different stabilizers to its amorphous form (Ibrahim et al. (2018)). KL could be assigned to two polymers, polyvinyl alcohol (PVA) and polyethylene glycol (PEG). The reflection at 19.7^O 2θ was due to the presence of crystalline PVA domains; the two reflections at 19° (hidden) and 22.9^O 2θ were due to the presence of crystalline PEG domains, as shown in Fig. 4. The XRPD of the FLZ nanosuspension stabilized with 5 % KL displayed the crystalline peaks of the drug. The obtained XRPD data of the FLZ nanosuspensions stabilized with higher KL concentrations showed that the FLZ showed a non-homogenous dispersion in the polymeric matrices and that FLZ had not transformed to an its amorphous form (Ibrahim, 2014). The X-ray diffraction spectrum of the XG formulations showed the presence of numerous distinct peaks, indicating that FLZ is a crystalline material with characteristic diffraction peaks which were observed their original positions but with slightly decreased intensities, which might have been due to the diluting effect of the stabilizing polymer, XG.

TEM was used to investigate the morphology of the prepared FLZ nanosuspensions. The F3 nanosuspension, which was stabilized with 5 % PLF127, was selected for the TEM study because of its particles being the smallest (192.9 ± 0.5 nm) and its zeta potential being the highest (−35.8 mV). In addition, the solubility of FLZ in this nanosuspension was higher (3.7 ± 0.81 mmol/L). Fig. 7 presents a TEM image of F3 (PLF 127 5 %), which is dark with nanosized spherical shapes, displaying the results obtained with this dynamic laser light scattering technique.

Ex vivo transcorneal permeation studies were performed to compare the corneal permeation of the prepared nanosuspension formulations containing FLZ. For each stabilizer, the nanosuspension with high drug solubility and small particles was selected. These formulations were F3 (stabilized with 5 % PLF 127), F4 (stabilized with 0.5 % KL), F7 (stabilized with 0.5 % HPMC), and F11 (stabilized with 1 % XG). The FLZ permeation results through the freshly excised goat corneas for the selected nanosuspensions are presented in Fig. 6 and Table 2. The highest cumulative drug permeation of the F4 nanosuspension containing KL might have been due its small particles (250.2 ± 0.17 nm) high zeta potential value (−21.4 mV), which produced improved transcorneal permeation (De Campos et al., 2001; Abdellatif et al., 2019). In addition, the solubility of the F4 nanosuspension containing KL was the highest at 6.8 ± 1.418 mmol/L.

The permeation parameters of FLZ, including the steady-state flux (J_{ss}), permeability coefficient (K_P), lag time, and cumulative amount permeated, were calculated using the ex vivo goat cornea permeation data (Abou El Ela et al., 2021). F4 had the highest permeability coefficient (52.126 cm/h x10^3), the highest cumulative amount of drug permeated (2841.45 ± 0.541 μg /cm^2), and the highest J_{ss} (260.63 ± 17.529). This could have been due to the F4 formulation having the highest solubility. The differences in the cumulative permeation

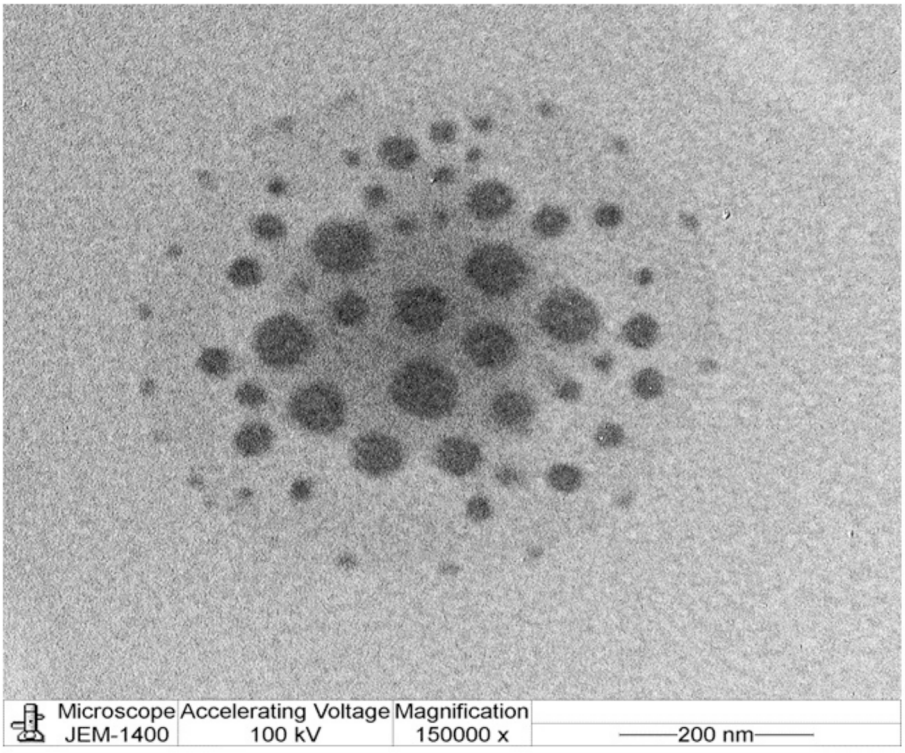

Fig. 7. TEM image of FLZ nanosuspension formulation F3.

parameters of nanosuspensions indicate the essential role of the stabilizers, which resulted in different corneal permeation profiles. According to the permeation parameters obtained, the FLZ nanosuspensions could be ranked in the following order: F4 (0.5 % KL) >, F11 (1 % XG) > F7 (0.5 % HPMC) > F3 (5 % PLF127).

5. Conclusions

We successfully used various concentrations of different stabilizers to prepare FLZ nanosuspension formulations. These stabilizers had varying effects on the particle size and zeta potential of the nanosuspensions depending on stabilizer concentration and type. The solubility of the nanosuspension formulations increased by up to 5.7 fold compared with that of the untreated drug. Variable amounts of FLZ were released from the nanosuspension formulations and permeated through goat corneas in an ex vivo experiment, which depended on the type of stabilizer used. As a result, we found that the FLZ in the nanosuspension stabilized with KL provided the highest extent of drug release, the largest flux, and the highest permeability coefficient, thereby increasing the ocular bioavailability of FLZ.

CRediT authorship contribution statement

Basmah N. Aldosari: Writing – original draft, Visualization, Funding acquisition. **Mohamed Abbas Ibrahim:** Visualization, Validation, Supervision, Resources, Methodology, Funding acquisition, Formal analysis, Data curation, Conceptualization. **Yara Alqahtani:** Resources, Methodology, Investigation, Data curation. **Amal El Sayeh F. Abou El Ela:** Writing – review & editing, Writing – original draft, Visualization, Supervision, Project administration, Methodology, Investigation, Data curation, Conceptualization.

Declaration of competing interest

The authors declare that they have no known competing financial interests or personal relationships that could have appeared to influence the work reported in this paper.

Acknowledgment

The authors extend their appreciation to the Researchers Supporting Project (RSP2024R171), King Saud University, Riyadh, Saudi Arabia.

Funding

The article after the pablication should include this Acknowledgement (The authors extend their appreciation to the Researchers Supporting Project (RSP2024R171), King Saud University, Riyadh, Saudi Arabia.)

References

Abdellatif, A.A.H., El-Telbany, D.F.A., Zayed, G., Al-Sawahli, M.M., 2019. Hydrogel containing PEG-coated Fluconazole nanoparticles with enhanced solubility and antifungal activity. J. Pharm. Innov. 14, 112–122. https://doi.org/10.1007/s12247-018-9335-z.

Abou El Ela, A.E.F., Ibrahim, M.A., Alqahtani, Y., Almomen, A., Aleanizy, F.S., 2021. Fluconazole nanoparticles prepared by antisolvent precipitation technique: Physicochemical, in vitro, ex vivo and in vivo ocular evaluation. Saudi Pharm. J. 29, 576–585. https://doi.org/10.1016/j.jsps.2021.04.018.

Alshora, D.H., Ibrahim, M.A., Elzayat, E., Almeanazel, O.T., Alanazi, F., 2018. Rosuvastatin calcium nanoparticles: Improving bioavailability by formulation and stabilization codesign. PLOS ONE 13, e0200218.

Alshora, D.H., Alsaif, S., Ibrahim, M.A., Ezzeldin, E., Almeanazel, O.T., El Ela, A.E.F., Ashri, L.Y., 2020. Co-stabilization of pioglitazone HCL nanoparticles prepared by planetary ball milling: in-vitro and in-vivo evaluation. Pharm. Dev. Technol. 25, 845–854. https://doi.org/10.1080/10837450.2020.1744163.

Chen, X., Matteucci, M.E., Lo, C.Y., Johnston, K.P., Williams III, R.O., 2009. Flocculation of polymer stabilized nanocrystal suspensions to produce redispersible powders. Drug Dev Ind. Pharm. 35, 283–296. https://doi.org/10.1080/03639040802282896.

Chowdhary, K.P., Madhav, B.L., 2005. Novel drug delivery technologies for insoluble drugs. Ind. Drugs. 42, 557–563.

Comba, S., Dalmazzo, D., Santagata, E., Sethi, R., 2011. Rheological characterization of xanthan suspensions of nanoscale iron for injection in porous media. J. Hazardous Materials. 185, 598–605. https://doi.org/10.1016/j.jhazmat.2010.09.060.

Comba, S., Sethi, R., 2009. Stabilization of highly concentrated suspensions of iron nanoparticles using shear-thinning gels of xanthan gum. Water Res. 43, 3717–3726. https://doi.org/10.1016/j.watres.2009.05.046.

De Campos, A.M., Sánchez, A., Alonso, M.a.J., 2001. Chitosan nanoparticles: a new vehicle for the improvement of the delivery of drugs to the ocular surface. Application to cyclosporin A. Int. J. Pharm. 224, 159–168. https://doi.org/10.1016/S0378-5173(01)00760-8.

Göğer, N.G., Aboul-Enein, H.Y., 2001. Quantitative determination of fluconazole in capsules and IV solutions by UV spectrophotometric methods. Anal. Lett. 34, 2089–2098. https://doi.org/10.1081/AL-100106841.

Gupta, S., Samanta, M.K., Raichur, A.M., 2010. Dual-drug delivery system based on in situ gel-forming nanosuspension of forskolin to enhance antiglaucoma efficacy. AAPS PharmSciTech. 11, 322–335. https://doi.org/10.1208/s12249-010-9388-x.

Helal, D.A., Abd EL-Rhman, D., Abdel-Halim, S.A., EL-Nabarawi, M.A., 2012. Formulation and evaluation of fluconazole topical gel. Int. J. Pharm. Pharm. Sci. 4, 176–183.

Ibrahim, M.A., 2014. Tenoxicam - Kollicoat IR® Binary Systems: physicochemical and biological evaluation. Acta Pol. Pharm. Drug Res. 71, 647–659.

Ibrahim, M.A., Shazly, G.A., Aleanizy, F.S., Alqahtani, F.Y., Elosaily, G.M., 2019. Formulation and evaluation of docetaxel nanosuspensions: In-vitro evaluation and cytotoxicity. Saudi. Pharm. J. 27, 49–55. https://doi.org/10.1016/j.jsps.2018.07.018.

Kabanov, A.V., Alakhov, V.Y., 2002. Pluronic block copolymers in drug delivery: From micellar nanocontainers to biological response modifiers. Crit. Rev. Ther. Drug Carrier Syst. 19, 1–72. https://doi.org/10.1615/CritRevTherDrugCarrierSyst.v19.i1.10.

Mahdy, R.A., Nada, W.M., Wageh, M.M., Kader, M.A., Saleh, M.M., Alswad, M.M., 2010. Assessment safety and efficacy of a combination therapy of topical amphotericin B and subconjunctival fluconazole for the treatment of fungal keratitis. Cutaneous and Ocular Toxicology. 29, 193–197. https://doi.org/10.3109/15569521003801454.

Muller, R.H., Jacobs, C., Kayser, O., 2000. Nanosuspensions for the formulation of poorly soluble drugs. Pharmaceutical emulsion sand suspensions. Marcel Dekker, New York.

Nutan, M.T.H., Reddy, I.K., 2010. General principles of suspensions. In: Kulshreshtha, A. K., Singh, O.N., Wall, G.M. (Eds.), Pharmaceutical suspensions: from formulation development to manufacturing. Springer, New York, pp. 52–55.

Pathak, M.K., Chhabra, G., Pathak, K., 2013. Design and development of a novel pH triggered nanoemulsified in-situ ophthalmic gel of fluconazole: Ex-vivo transcorneal permeation, corneal toxicity and irritation testing. Drug Development and Industrial Pharmacy. 39, 780–790. https://doi.org/10.3109/03639045.2012.707203.

Patravale, V., Date, A.A., Kulkarni, R., 2004. Nanosuspensions: a promising drug delivery strategy. J. Pharm. Pharmacol. 56, 827–840. https://doi.org/10.1211/0022357023691.

Ramezani, V., Vatanara, A., Najafabadi, A.R., Moghaddam, S.P.H., 2014. Clarithromycin dissolution enhancement by preparation of aqueous nanosuspensions using sonoprecipitation technique. Iran. J. Pharm. Res. 13, 809–818.

Savjani, K.T., Gajjar, A.K., Savjani, J.K., 2012. Drug solubility: importance and enhancement techniques. ISRN Pharmaceutics. 1–11 https://doi.org/10.5402/2012/195727.

Sayed, E.G., Hussein, A.K., Khaled, K.A., Ahmed, O.A., 2015. Improved corneal bioavailability of ofloxacin: biodegradable microsphere-loaded ion-activated in situ gel delivery system. Drug Design. Develop. Therapy. 9, 1427–1435. https://doi.org/10.2147/DDDT.S80697.

Sezgin, Z., Yüksel, N., Baykara, T., 2006. Preparation and characterization of polymeric micelles for solubilization of poorly soluble anticancer drugs. Eur. J. Pharm Biopharm 64, 261–268. https://doi.org/10.1016/j.ejpb.2006.06.003.

Suzuki, H., Miyamoto, N., Masada, T., Hayakawa, E., Ito, K., 1996. Solid dispersions of benidipine hydrochloride. II. Investigation of the interactions among drug, polymer and solvent in preparations. Chem. Pharm. Bull. 44, 372–377.

Wadhwa, S., Paliwal, R., Paliwal, S.R., Vyas, S., 2009. Nanocarriers in ocular drug delivery: an update review. Current Pharm. Design. 15, 2724–2750. https://doi.org/10.2174/138161209788923886.

Wang, Y., Zheng, Y., Zhang, L., Wang, Q., Zhang, D., 2013. Stability of nanosuspensions in drug delivery. J. Control. Release. 172, 1126–1141. https://doi.org/10.1016/j.jconrel.2013.08.006.

Xue, D., Sethi, R., 2012. Viscoelastic gels of guar and xanthan gum mixtures provide long-term stabilization of iron micro-and nanoparticles. J. Nanopart. Res. 14, 1239. https://doi.org/10.1007/s11051-012-1239-0.

Yilmaz, S., Maden, A., 2005. Severe fungal keratitis treated with subconjunctival fluconazole. Amer. J. Ophthalmol. 140 (454), e451–e454. E458. https://doi.org/10.1016/j.ajo.2005.03.074.

Zimmer, A., Kreuter, J., 1995. Microspheres and nanoparticles used in ocular delivery systems. Advan. Drug Deliv. Reviews 16, 61–73.

Zu, S., Yang, L., Huang, J., Ma, C., Wang, W., Zhao, C., Zu, Y., 2012. Micronization of taxifolin by supercritical antisolvent process and evaluation of radical scavenging activity. Int. J. Mol. Sci. 13, 8869–8881. https://doi.org/10.3390/ijms13078869.